

Model studies of the propagation of errors during the inversion of 2D resistivity data recorded with the Wenner (α) geometry along curved and angled survey lines

François Fourie¹

1. Orpheus Hydrogeophysics, South Africa, FDFourie@OrpheusHGP.co.za

ABSTRACT

When recording 2D resistivity data along curved or angled survey lines, the recorded apparent resistivity data will be affected by the fact that the true geometric factors will differ from the assumed geometric factors of a straight survey line. Numerical model studies show that, although the errors in the apparent resistivities may be small even for large angles and curvatures, these errors may rapidly increase in magnitude during inversion. This is particularly true during the inversion of data recorded along angled survey lines where input errors may increase by an order of magnitude within a couple of iterations. Although it seems that angles should be avoided in favour of curves when it is not possible to perform a resistivity survey along a straight line, the apparent resistivity data recorded along an angled survey line may very readily be corrected prior to inversion if the true electrode positions can be measured.

Keywords: Error propagation, 2D resistivity, inversion, curved/angled survey lines

INTRODUCTION

Various multi-electrode 2D resistivity systems employ instrument protocols that control switching between the different electrode pairs during measurement. These protocols normally assume that the survey lines are straight. However, when survey lines are curved or angled, the calculated apparent resistivities may be affected by fact that the true (field) geometric factors could differ from the assumed (instrument) geometric factors.

In this paper I examine how the errors in the calculated apparent resistivities may be propagated in magnitude and spatially during inversion. The investigation is related to the study of the effects of in-line and off-line electrode misplacements at individual electrodes as described by Zhou and Dahlin (2003). These authors showed that the change to the geometric factors is much smaller for off-line spacing errors than for in-line spacing errors. They found that certain electrode geometries (e.g. the dipole-dipole, γ - and Wenner (β) arrays) are more sensitive to spacing errors than others. For these geometries an in-line spacing error of 10% may lead to relative errors in excess of 20% in the calculated pseudo-sections. Furthermore, the errors in the pseudo-sections were found to cause artefacts in the inverted resistivity models.

Whereas Zhou and Dahlin (2003) considered the effects of errors at individual electrodes, this paper focuses on the effects of systematic electrode "misplacements" along curved and angled survey lines. This is done by:

- 1) Calculating forward models for particular resistivity distributions,
- 2) Adjusting the modelled apparent resistivity values to those values that would have been recorded along curved/angled survey lines, and,
- 3) Inverting the modified resistivity pseudo-sections.

Comparison of the inverted resistivity models of curved/angled survey lines to those of straight lines at particular iterations in the inversion process is done to isolate the errors in the modelled resistivity sections that are due to the introduction of the systematic errors in the apparent resistivity values. This is done to empirically evaluate the impact and significance of error propagation, both in magnitude and spatially.

MODEL STUDIES

The Wenner (α) geometry with outer current electrodes and inner potential electrodes is used for all model studies in this paper. In order to investigate the effects of different resistivity distributions on error propagation during inversion, five models are considered, namely:

- 1) Model A – a homogeneous half-space with a resistivity of 100 Ωm ,
- 2) Model B – a two-layer earth consisting of a 10 m thick layer with resistivity 10 Ωm overlying a half-space with a resistivity of 100 Ωm ,

- 3) Model C – a two-layer earth consisting of a 10 m thick layer with resistivity 100 Ωm overlying a half-space with a resistivity of 10 Ωm ,
- 4) Model D – a two-layer earth consisting of a 10 m thick layer with resistivity 20 Ωm overlying a half-space with a resistivity of 40 Ωm , and,
- 5) Model E – a two-layer earth consisting of a 10 m thick layer with resistivity 40 Ωm overlying a half-space with a resistivity of 20 Ωm .

Models B and C were selected to represent high contrast models while Models D and E represent low contrast models.

The forward responses of the two-layer models were obtained by using the software package RES1D to calculate the one-dimensional vertical (sounding) responses of each model for the Wenner (α) array and by applying these responses to all the measurement positions to obtain resistivity pseudo-sections. The apparent resistivity values were then adjusted to correspond to those values that would have been recorded along curved/angled survey lines by multiplication with the factor K'/K , where K' is the geometric factor for electrode positions along the curved/angled survey line and K is the corresponding geometric factor for the straight electrode geometry.

The adjusted resistivity pseudo-sections used as inputs to the inversion process were calculated for 100 electrode positions with a standard electrode spacing (s) of 1 m. Apparent resistivity values were calculated for 33 different depths of investigation corresponding to electrode separations of is where i is an integer representing the number of standard electrode spacings between “active” electrodes during a particular measurement ($1 \leq i \leq 33$). The total number of data points in the pseudo-sections was therefore 1,617.

The resistivity pseudo-sections were inverted with the software package RES2DINV (Loke, 2004) which uses algorithms based on the smoothness-constrained least-squares method (deGroot-Hedlin and Constable, 1990; Sasaki, 1992).

To allow comparison of the propagated errors along curved and angled survey lines, angles for which the curved and angled survey lines have similar “curvatures” were considered. In Figure 1 a curved and an angled survey line of which the first and last electrodes (numbered 1 and m) and centre positions coincide are shown. For this geometry $\theta_A = 0.5\theta_C$. The forward models of the angled survey lines were calculated for angles (θ_A) of $\pi/12$, $\pi/6$ and $\pi/4$ radians. These responses were compared with the responses obtained along curved survey lines with angles (θ_C) of $\pi/6$, $\pi/3$ and $\pi/2$ radians, respectively.

Examples of the input error distribution in the pseudo-sections are shown in Figure 12 and Figure 13 for a curved survey line ($\theta_C = \pi/2$ radians) and an angled survey line ($\theta_A = \pi/4$ radians), respectively. As

expected, the errors for the curved survey line are constant for a specific electrode spacing (constant i) but increase with increasing i as the degree of non-collinearity between the electrode pairs increases. The errors attain maximum values of approximately 2.5% for the largest electrode spacing.

For the angled survey line the errors are greatest for measurements where the electrode pairs are located symmetrically around the position of the angle in the survey line and attain maximum values of approximately 6.5%. A significant number (51%) of the resistivity values in the pseudo-section are affected by the presence of the angle in the survey line.

MODEL RESULTS

The maximum errors in the inverted resistivity models (i.e. the maximum differences between the inverted models along curved/angled survey lines and the inverted models along straight survey lines) are shown in Figure 2 to Figure 6 for curved survey lines on Models A to E, while Figure 7 to Figure 11 show the corresponding errors due to angled survey lines. The maximum errors are plotted against iteration number for a total of eight iterations. The following observations may be made from these figures:

- The magnitudes of the errors observed during inversion are model dependent,
- The maximum errors generally increase (are propagated in magnitude) with the number of iterations, although this behaviour is not observed in all models (see for example Figure 4),
- Increasing angles and curvatures lead to larger errors in the inverted models, and,
- The maximum errors are significantly smaller for curved survey lines than for angled survey lines.

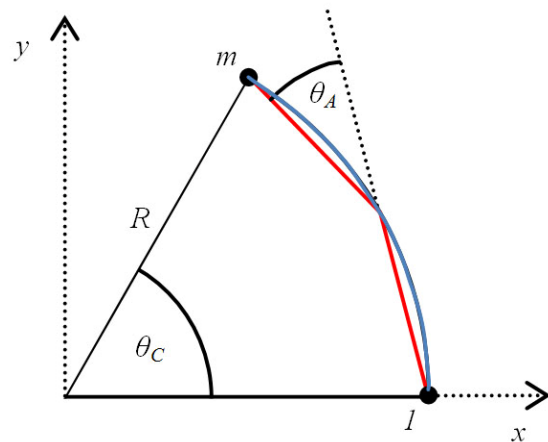


Figure 1. Curved (blue) and angled (red) survey lines with a similar “curvature”.

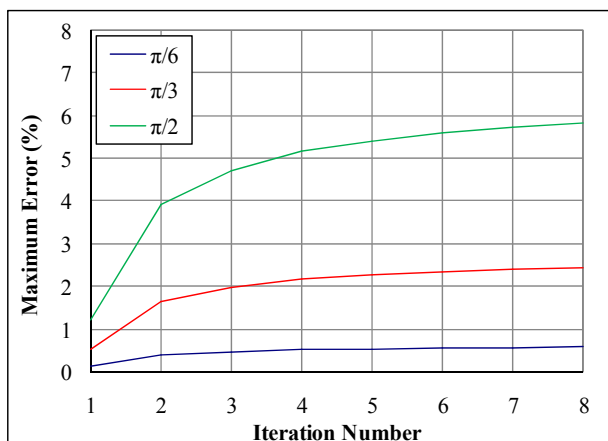


Figure 2. Maximum errors observed during the inversion of resistivity data calculated for a curved survey line over a half-space (Model A, $\rho = 100 \Omega\text{m}$).

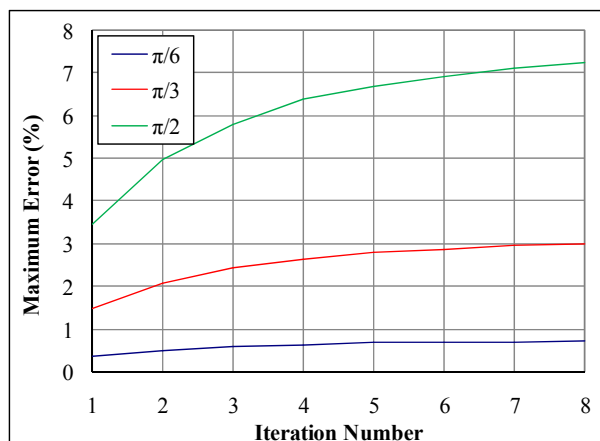


Figure 5. Maximum errors observed during the inversion of resistivity data calculated for a curved survey line over a two-layer earth (Model D, $\rho_1 = 20 \Omega\text{m}$, $h_1 = 10\text{m}$, $\rho_2 = 40 \Omega\text{m}$).

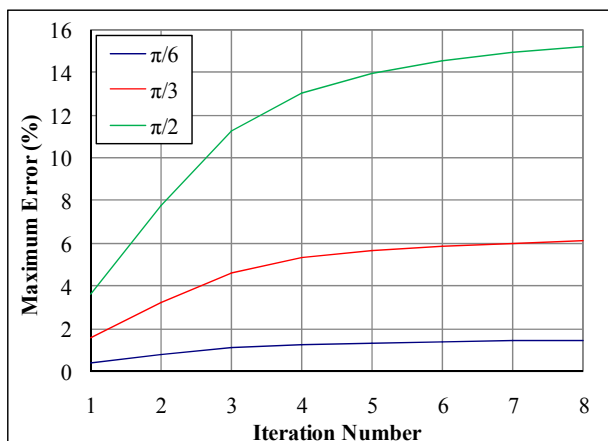


Figure 3. Maximum errors observed during the inversion of resistivity data calculated for a curved survey line over a two-layer earth (Model B, $\rho_1 = 10 \Omega\text{m}$, $h_1 = 10\text{m}$, $\rho_2 = 100 \Omega\text{m}$).

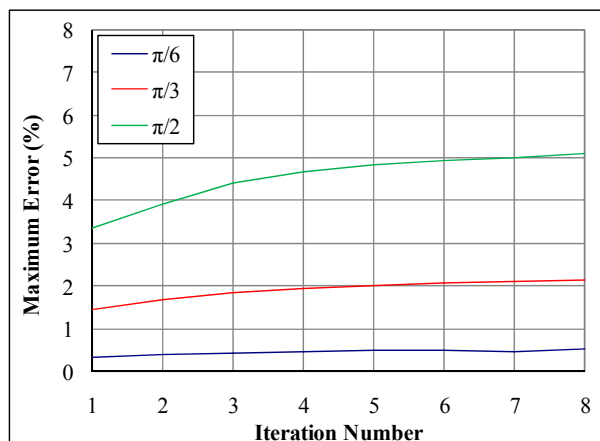


Figure 6. Maximum errors observed during the inversion of resistivity data calculated for a curved survey line over a two-layer earth (Model E, $\rho_1 = 40 \Omega\text{m}$, $h_1 = 10\text{m}$, $\rho_2 = 20 \Omega\text{m}$).

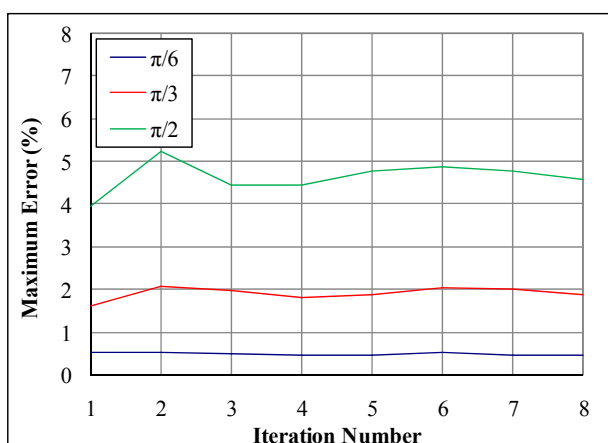


Figure 4. Maximum errors observed during the inversion of resistivity data calculated for a curved survey line over a two-layer earth (Model C, $\rho_1 = 100 \Omega\text{m}$, $h_1 = 10\text{m}$, $\rho_2 = 10 \Omega\text{m}$).

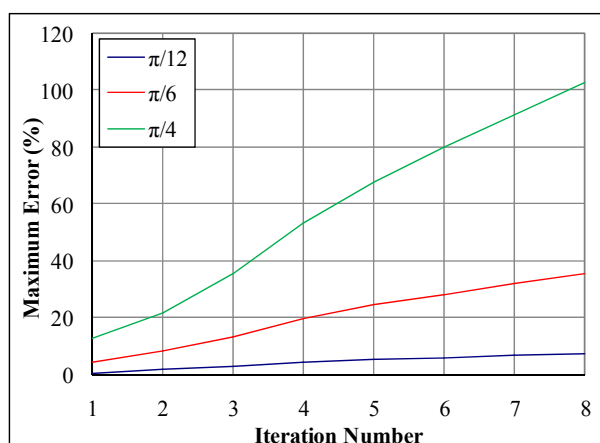


Figure 7. Maximum errors observed during the inversion of resistivity data calculated for an angled survey line over a half-space (Model A, $\rho = 100 \Omega\text{m}$).

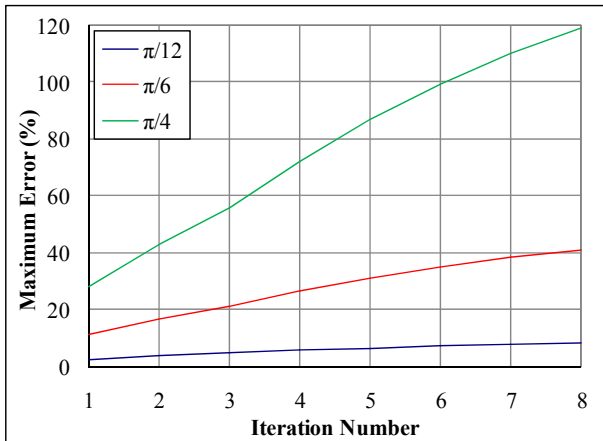


Figure 8. Maximum errors observed during the inversion of resistivity data calculated for an angled survey line over a two-layer earth (Model B, $\rho_1 = 10 \Omega\text{m}$, $h_1 = 10\text{m}$, $\rho_2 = 100 \Omega\text{m}$).

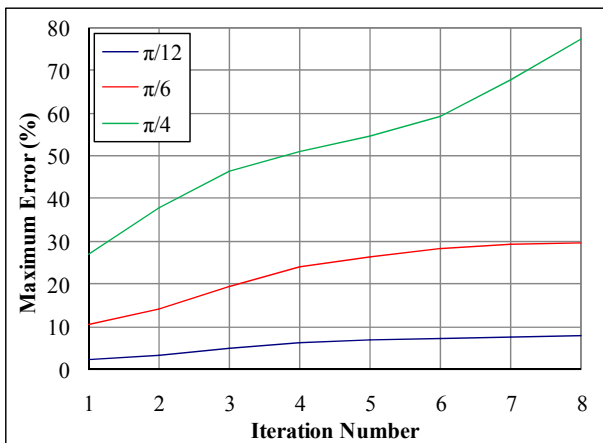


Figure 9. Maximum errors observed during the inversion of resistivity data calculated for an angled survey line over a two-layer earth (Model C, $\rho_1 = 100 \Omega\text{m}$, $h_1 = 10\text{m}$, $\rho_2 = 10 \Omega\text{m}$).

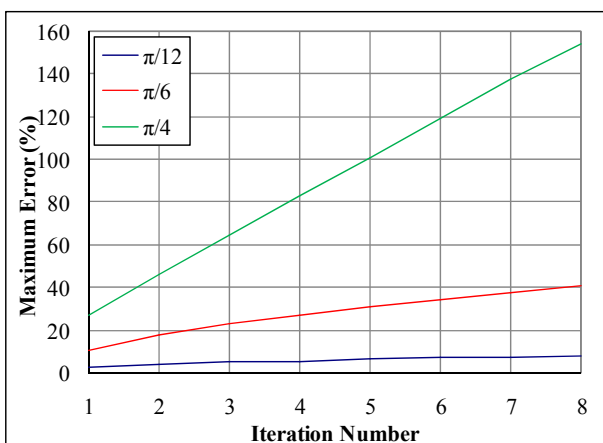


Figure 10. Maximum errors observed during the inversion of resistivity data calculated for an angled survey line over a two-layer earth (Model D, $\rho_1 = 20 \Omega\text{m}$, $h_1 = 10\text{m}$, $\rho_2 = 40 \Omega\text{m}$).

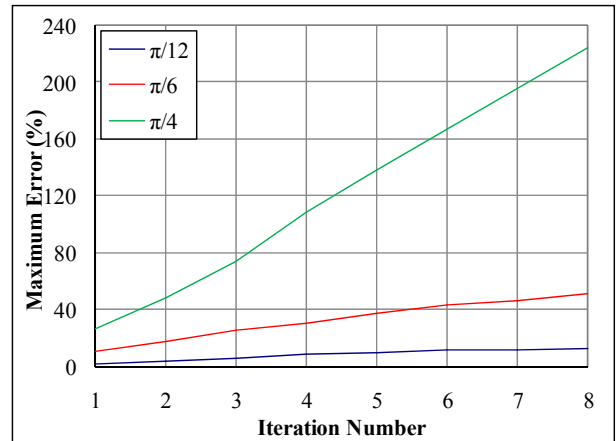


Figure 11. Maximum errors observed during the inversion of resistivity data calculated for an angled survey line over a two-layer earth (Model E, $\rho_1 = 40 \Omega\text{m}$, $h_1 = 10\text{m}$, $\rho_2 = 20 \Omega\text{m}$).

The results of the model studies are summarised in Table 1 for the fourth iteration of inversion. For comparison, the maximum errors in the apparent resistivities of the input models are also listed. It is seen that even though curved and angled survey lines may result in relatively small errors in the apparent resistivity values, the errors may be rapidly propagated (in magnitude) during inversion and could result in distorted resistivity models. This is particularly true for data recorded along angled survey lines.

As an example of how error propagation can affect the spatial distribution of resistivities in the modelled resistivity sections, consider Figure 14 to Figure 18. Figure 14 is the inverted resistivity model obtained after the fourth iteration of least-squares inversion of the apparent resistivity data recorded along a straight survey line on a two-layer earth with $\rho_1 = 10 \Omega\text{m}$, $h_1 = 10\text{m}$ and $\rho_2 = 100 \Omega\text{m}$. Due to the general problem of non-uniqueness in inversion, the modelled resistivity section does not clearly resolve the contact between the two layers, but displays a gradual increase in the resistivities for depths larger than approximately 8 m.

Figure 15 displays the inverse model for data along a curved ($\theta_C = \pi/2$ radians) survey line. Comparison of Figure 15 with Figure 14 shows that the inverse model of the curved survey line is at first glance almost indistinguishable from the inverse model of the straight survey line. There is, however, a significant difference between the inverse models of the angled ($\theta_A = \pi/4$ radians, Figure 16) and straight survey lines. The differences between the modelled resistivity sections along the curved and angled survey lines and the straight survey line are shown in Figure 17 and Figure 18, respectively. It is seen that both curved and angled resistivity models slightly under- and overestimate the resistivities at some positions at shallow depths, but overestimate the resistivities at larger depths near the centres of the modelled sections. The differences are, however, much more pronounced for the model of the angled survey line.

Table 1. Maximum errors in the modelled resistivities after the fourth iteration.

Iteration 4						
Curved survey lines						
θ_C (rad)	Max. Err. in App. Res. (%)	Max. Error in Modelled Resistivity (%)				
		Model				
		A	B	C	D	E
$\pi/6$	0.21	0.53	1.28	0.47	0.63	0.48
$\pi/3$	1.06	2.17	5.35	1.82	2.65	1.93
$\pi/2$	2.48	5.19	13.08	4.44	6.38	4.67
Angled survey lines						
θ_A (rad)	Max. Err. in App. Res. (%)	Max. Error in Modelled Resistivity (%)				
		Model				
		A	B	C	D	E
$\pi/12$	0.57	4.33	5.91	6.35	5.59	8.81
$\pi/6$	2.20	19.91	26.52	24.18	27.33	31.02
$\pi/4$	6.37	53.28	72.36	51.17	83.09	108.75

CONCLUSIONS

Although the errors in the apparent resistivities recorded along curved and angled survey lines may be relatively small (less than 2.5% for a curved survey line with of curvature of less than $\pi/2$ radians and less than 6.5% for an angled survey line with an angle of less than $\pi/4$ radians), these errors may be rapidly propagated in magnitude during inversion and could result in distorted

resistivity models. The errors made along angled survey lines are particularly prone to propagation and may increase by an order of magnitude within a couple of iterations. This observation suggests that, if not possible to record 2D resistivity data along straight survey lines, one should avoid angles and rather work along curves. However, if the true surface positions of the electrodes can be measured (for example with a differential GPS), the apparent resistivity data recorded along an angled survey line may readily be corrected prior to inversion by multiplication with the ratio of the geometric factors of the angled and straight survey lines (K'/K) in order to reduce or eliminate the input errors.

REFERENCES

deGroot-Hedlin, C., and Constable, S., 1990, Occam's inversion to generate smooth, two-dimensional models from magnetotelluric data: *Geophysics* 55, 1613-1624.

Loke, M.H., 2004, Rapid 2-D Resistivity & IP inversion using the least-squares method: Geotomo Software, Malaysia.

Sasaki, Y., 1992, Resolution of resistivity tomography inferred from numerical simulation: *Geophysical Prospecting* 40, 453-464.

Zhou, B., Dahlin, T., 2003, Properties and effects of measurement errors on 2D resistivity imaging surveying: *Near Surface Geophysics* 1, 105-117.

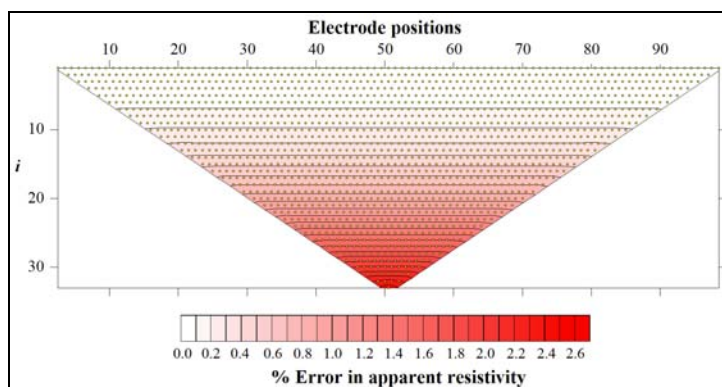


Figure 12. The percentage error in the calculated apparent resistivity: curved survey line, $\theta_C = \pi/2$ radians.

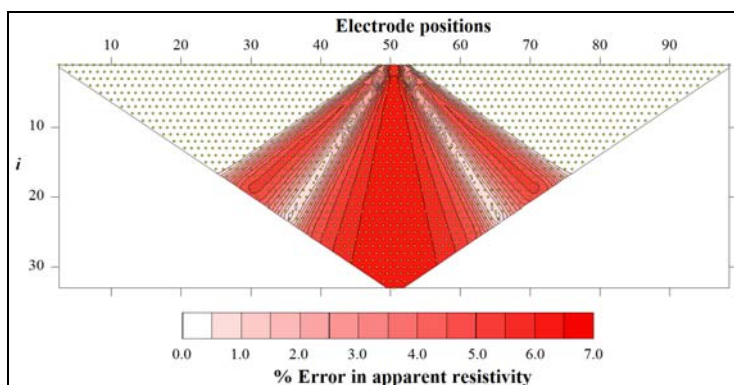


Figure 13. The percentage error in the calculated apparent resistivity: angled survey line, $\theta_A = \pi/4$ radians.

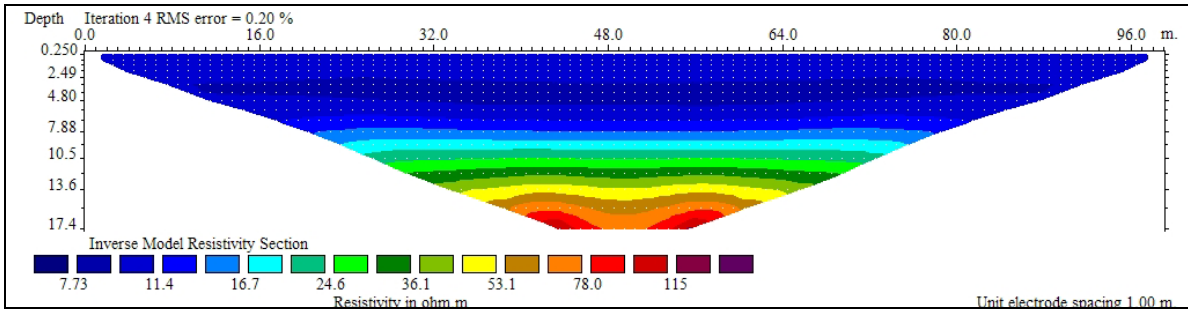


Figure 14. Modelled resistivity section for a straight survey line (Model B, $\rho_1 = 10 \Omega\text{m}$, $h_1 = 10\text{m}$, $\rho_2 = 100 \Omega\text{m}$).

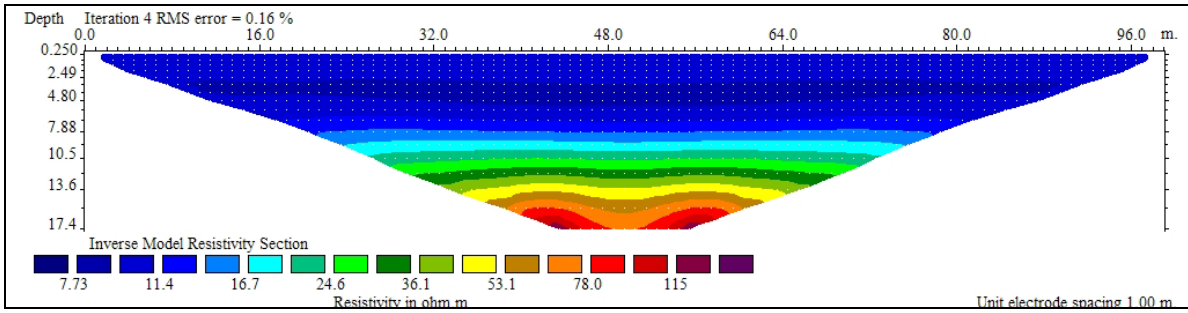


Figure 15. Modelled resistivity section for a curved survey line (Model B, $\rho_1 = 10 \Omega\text{m}$, $h_1 = 10\text{m}$, $\rho_2 = 100 \Omega\text{m}$, $\theta_C = \pi/2$ radians).

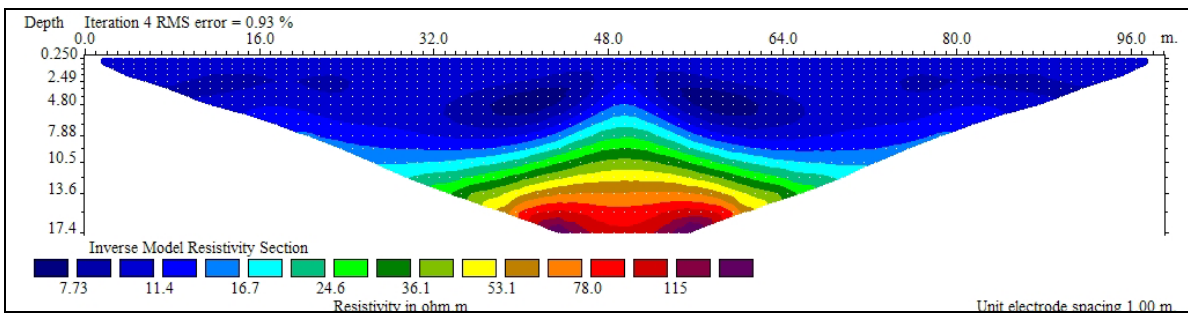


Figure 16. Modelled resistivity section for an angled survey line (Model B, $\rho_1 = 10 \Omega\text{m}$, $h_1 = 10\text{m}$, $\rho_2 = 100 \Omega\text{m}$, $\theta_A = \pi/4$ radians)

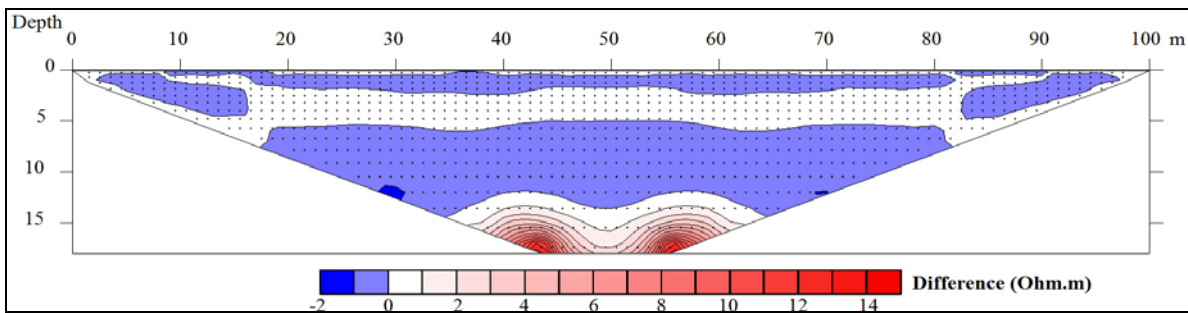


Figure 17. Difference between the resistivity models of the curved and straight survey lines.

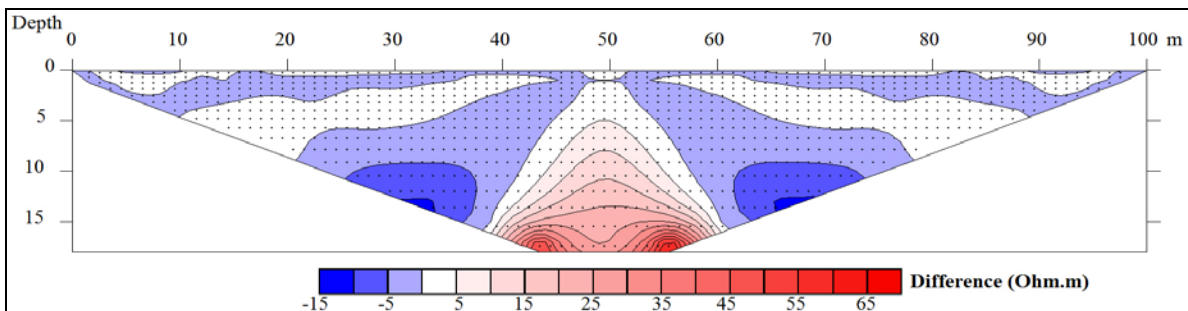


Figure 18. Difference between the resistivity models of the angled and straight survey lines.